High resolution electron energy loss spectroscopy of manganese oxides: Application to Mn_3O_4 nanoparticles

L. Laffont[a,*], *P. Gibot*[b]

[a]*Institut Carnot, Laboratoire CIRIMAT (équipe MEMO), CNRS UMR 5085, ENSIACET, 4 allée Emile Monso, BP 74233, 31432 Toulouse cedex 4, France*

[b]*Laboratoire de Réactivité et Chimie des Solides CNRS UMR 6007, Université de Picardie Jules Verne, 33 rue Saint Leu, 80039 Amiens cedex 9, France*

A B S T R A C T

Manganese oxides particularly Mn_3O_4 Hausmannite are currently used in many industrial applications such as catalysis, magnetism, electrochemistry or air contamination. The downsizing of the particle size of such material permits an improvement of its intrinsic properties and a consequent increase in its performances compared to a classical micron-sized material. Here, we report a novel synthesis of hydrophilic nano-sized Mn_3O_4, a bivalent oxide, for which a precise characterization is necessary and for which the determination of the valency proves to be essential. X-ray diffraction (XRD), Transmission Electron Microscopy (TEM) and particularly High Resolution Electron Energy Loss Spectroscopy (HREELS) allow us to perform these measurements on the nanometer scale. Well crystallized 10–20 nm sized Mn_3O_4 particles with sphere-shaped morphology were thus successfully synthesized. Meticulous EELS investigations allowed the determination of a Mn^{3+}/Mn^{2+} ratio of 1.5, i.e. slightly lower than the theoretical value of 2 for the bulk Hausmannite manganese oxide. This result emphasizes the presence of vacancies on the tetrahedral sites in the structure of the as-synthesized nanomaterial.

Keywords:
EEL spectroscopy
Manganese oxides
Mn_3O_4 nanoparticles

1. Introduction

Electron Energy Loss Spectroscopy (EELS), which enables the electronic density of states to be probed at a nanometer scale, is a powerful technique to study the chemical state of transition metal oxides in nano-powders or inhomogeneous materials [1,2]. Furthermore, the combination of a high resolution electron energy loss spectrometer (HREELS) with a transmission electron microscope (TEM) exhibits the advantage of high lateral resolution for chemical analysis and for structural determination by means of electron diffraction and high resolution imaging. This aspect is very promising for scientists who are constantly searching for better structural and chemical characterizations of nano-sized manganese oxides.

Manganese oxide as Mn_3O_4 has been synthesized [3] and the determination of the oxidation states of nano-sized manganese sample is essential to their use in battery materials.

In this paper the degree of crystallinity and the grain size distribution of Mn_3O_4 will be studied by X-ray diffraction (XRD), nitrogen adsorption (BET measurements) and high resolution transmission electron microscopy (HRTEM) characterizations. We also investigate the oxidation state of manganese oxides, i.e. indirectly the oxygen stoichiometry, in these materials at the nanometer scale by means of electron energy loss spectroscopy.

We first present the nanotextural characterization of Mn_3O_4 and in the second part an EELS study of the Mn–$L_{2,3}$ and O–K edges from a set of reference manganese oxides: MnO

* *Corresponding author*. Tel.: +33 5 34323437; fax: +33 5 3432343.
E-mail address: Lydia.laffont@ensiacet.fr (L. Laffont).

doi:10.1016/j.matchar.2010.09.001

(Face-centred cubic structure, space group $Fm\bar{3}m$), Mn_2O_3 (cubic structure, space group $Ia\bar{3}$), Mn_3O_4 (tetragonal structure, space group $I4_1/amd$) and MnO_2 (tetragonal structure, space group $P4_2/mnm$). These reference EELS spectra are essential to determine the oxidation states of the as-made material Mn_3O_4.

2. Experimental Section

The reference manganese oxides as MnO, Mn_2O_3, Mn_3O_4 and MnO_2 were purchased from Aldrich and checked by X-ray diffraction.

2.1. *Synthesis of Mn_3O_4*

Absolute ethanol, potassium permanganate $KMnO_4$ (99+%), and monohydrate hydrazine $N_2H_4.H_2O$ (98%), were purchased from Aldrich Chemical Co. Sodium dodecylsulphate (SDS) was obtained from Acros Organics. The complete procedure for the synthesis of hydrophilic Mn_3O_4 was elsewhere described [3] but it can be briefly summarised as follows. In a typical synthesis, 0.4 mmol of $KMnO_4$ and 0.4 mmol of sodium dodecylsulphate (SDS) were dissolved in 20 ml of distilled water. Then, 20 ml of an aqueous solution of monohydrate hydrazine (4 mmol) was injected rapidly to the solution under vigorous magnetic stirring. The colour of the solution immediately turned from dark purple to black/brown then to orange/brown. The resulting solution was stirred for 1 h at 70 °C and then cooled down to room temperature. The orange/brown material was precipitated or separated via centrifugation. The solid was washed twice with distilled water then once with ethanol and dried at 50 °C overnight.

2.2. *Nanoparticles Characterization*

The X-ray powder diffraction (XRD) pattern of the hydrophilic Mn_3O_4 particles thus prepared was collected on a Philips PW 1830 diffractometer operating with a Cu Kα radiation ($\lambda = 1.54056$ Å) at 40 kV and 30 mA. The Full Proof Suite of the WinPLOTR software was used to determine the crystallographic data of the as-made samples. A LaB_6 powder was analyzed as reference to correct for instrumental broadening. Nitrogen absorption measurement was performed on a Micromeritics ASAP 2020 at 77 K on a sample (of approximately 0.200 g) previously outgassed at 393 K for 12 h. The specific surface area (S_{BET}) was determined according to the Brunauer–Emmet–Teller (BET) method in the 0.02–0.25 relative pressure range. The error on the measurement, given by the manufacturer is less than 2%. TEM and HRTEM imaging were performed using a FEI Tecnai F20 S-Twin electron microscope operating at 200 kV. The diffraction patterns were obtained using the selected area electron diffraction (SAED) mode or by Fourier transform of the HRTEM image. For EELS analysis, the high energy resolution spectra were acquired at the National Centre for HREM at the Delft University of Technology, The Netherlands, on a FEI TECNAI microscope operating at 200 keV equipped with a Wien-filter monochromator, an improved high tension tank and a high resolution GIF (HR-GIF). Measurements were made at a total energy resolution of 0.25 eV, determined by measuring the full width at half maximum of the zero-loss peak. After some tuning, the following conditions were chosen for the EEL spectra acquisition: an illumination semi-angle α of 1.9 mrad, a collection semi-angle β of 3.8 mrad, and an energy dispersion of 0.05 eV/channel. The energy positions of the Mn–$L_{2,3}$ and O–K were accurately determined using the internal calibration system based on the electrostatic drift tube of the EEL spectrometer followed by a fine calibration based on well-known standard position of edge of transition metal. The accuracy of calibration is of about 0.06%.

3. Results and Discussion

3.1. *Mn_3O_4 Characterization*

Fig. 1 shows the XRD pattern of the hydrophilic pristine manganese-based product. All diffraction peaks can be indexed, as described in the 24-0734 JCPDS card characteristic of the Mn_3O_4 Hausmannite, in a centered tetragonal structure with a $I4_1/amd$ space group. No secondary phase was detected on the present diffractogram. The full pattern matching refinement realized on this pattern [3] allowed the lattice parameters to be estimated as equal to $a = 5.7669(4)$ Å, $c = 9.4506(4)$ Å and $V = 314.30(5)$ Å^3 ($R_{wp} = 10.1$–$R_{exp} = 8.75$). The crystallite size of the pristine Mn_3O_4 calculated from the refinement was 147.50 Å with a standard deviation of ±16.25 Å; nano-dimension predicted by the broadening nature of the diffraction peaks. The weak standard deviation also revealed that the crystallite morphology might be assimilated to a nano-sphere.

The morphology and structure of the pristine Mn_3O_4 sample were investigated by HRTEM and SAED techniques; the corresponding images are shown in Fig. 2. In Fig. 2(a), the hydrophilic pristine Mn_3O_4 sample consists of sphere-shaped particles that have an average diameter of 10–20 nm. This value is very similar to the crystallite size deduced by X-ray refinements, i.e. 14.75 nm, which suggests the monocrystalline nature of the particles. The morphology of the nanoparticles determined by HRTEM studies (Fig. 2(b)) also confirms the deduction made from XRD; i.e. a spherical shape of Mn_3O_4 particles. The images exhibit a relative agglomeration of the nanoparticles due to their ultra fine size and on some of these particles, diffraction planes can be observed which emphasize the good crystallinity of the sample (Fig. 2b). The SAED pattern of the manganese-based nano-sized particles is presented in Fig. 2(a-inset) and obvious diffraction rings can be found. These rings can be attributed successively to the (112), (103), (211), (220), (105) and (224) Miller planes which well characterise the tetragonal Mn_3O_4 structure within a $I4_1/amd$ space group.

In order to get more information about the pristine product, the BET specific surface area of the powder (S_{BET}) was performed by nitrogen adsorption and the following equation was used to deduce the particle size: $\varnothing = 6/(\rho \times S_{BET})$; where ρ corresponds to the density of the powder (4876 kg m^{-3}). This equation could be used because of the spherical shape of the particles and the assumption of a monodispersed powder. The

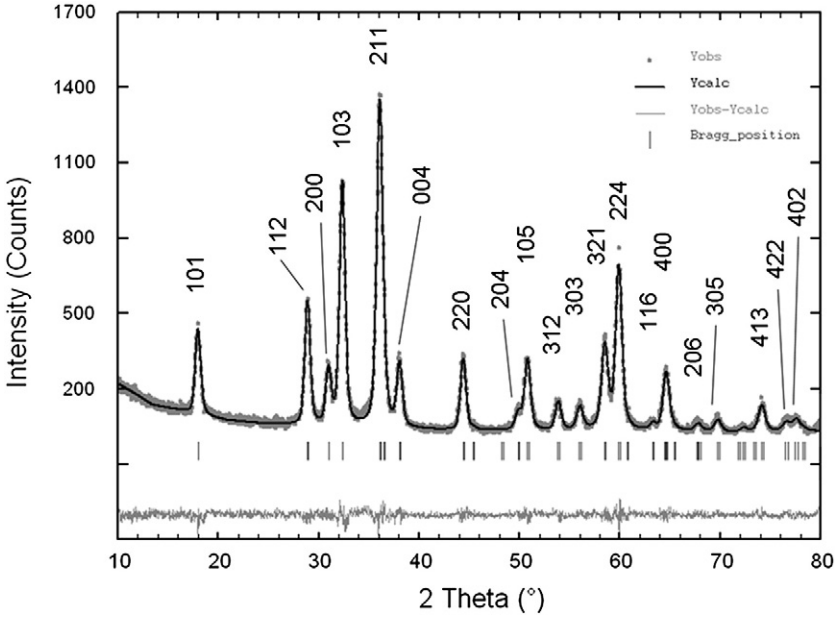

Fig. 1 – XRD pattern of the pristine hydrophilic Mn_3O_4 powder.

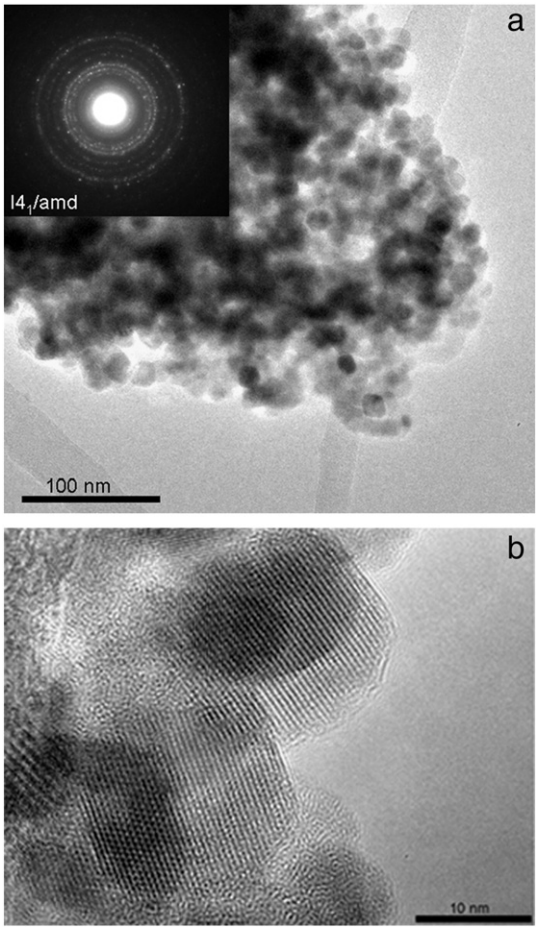

Fig. 2 – TEM combined with SAED pattern (a) and HRTEM (b) images of the pristine Mn_3O_4 nanopowder.

hydrophilic Mn_3O_4 powder has revealed values of 68.1 ± 1.4 $m^2 g^{-1}$ and 18.09 ± 0.36 nm sized for the specific surface area and the particle size, respectively. This size of particles is consistent with the X-ray and HRTEM results. To check the valency of this synthesized Mn_3O_4, EEL spectroscopy was investigated.

3.2. *EELS Spectra*

Fig. 3 shows the oxygen K-edge spectra after background subtraction for four reference oxide spectra (MnO_2, Mn_2O_3, Mn_3O_4 bulk and MnO) and the investigated hydrophilic Mn_3O_4

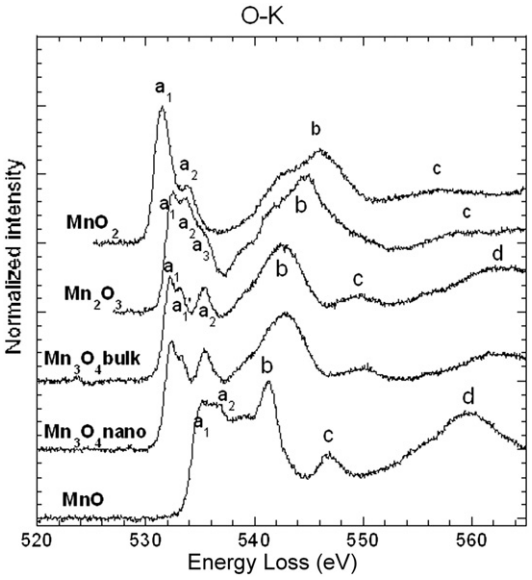

Fig. 3 – Oxygen K-edge spectra from five studied oxides after deconvolution of multiple loss events and background subtraction.

(labelled in the following "nano-Mn_3O_4"). The fine structure of the manganese oxides is consistent with the previous data reported by Garvie et al. [4]. Fine structures on the oxygen K edge can be interpreted in terms of transition processes governed by the dipole selection rule ($\Delta l = \pm 1$). Four main peaks are identified in each spectrum (a–d), the positions of which are listed in Table 1. The first peak, the pre-peak (a) around 530 eV has been attributed to transitions from 1s core states to oxygen 2p states hybridized with manganese 3d orbitals [5,6]. One notes the splitting on peak (a) for all the manganese oxides. De Groot et al. have pointed out that the pre-peak region may consist of one or several peaks which can be interpreted in terms of the ligand field and exchange splitting [6]. The O–K edge of MnO has been satisfactorily explained by multiple scattering calculations by using a cluster size of 7 shells [4]. The second peak (b) at 5–10 eV above threshold is related to the projected unoccupied oxygen p states mixed with the manganese 4sp band at higher energy above the Fermi level [6]. The third region extending up to 30–50 eV above threshold including peaks (c) and (d) can be interpreted in terms of the multiple scattering of the excited electron with low kinetic energy. More precisely, peaks (c) and (d) arise from multiple scattering within oxygen shells of increased size around the excited atom [7] and their peak positions can be correlated to the interatomic distances between oxygen atoms through the resonance condition [8].

Fig. 4 shows the manganese $L_{2,3}$ edge spectra from these five studied oxides after background subtraction. They consist of two white lines L_3 and L_2 due to the transitions from $2p_{3/2}$ and $2p_{1/2}$ core states to 3d unoccupied states localized on the excited manganese ions. These peaks are separated by the spin–orbit interaction of core states which has been found independent of the oxidation states of manganese ions. The L_3 peak position tends to shift to higher energy as the formal valence of manganese ion is increased (Table 2), which is consistent with the results of previous researchers [9]. The ratio of the integrated intensities of the L_3 and L_2 white lines (L_3/L_2) can be correlated to the valency of the transition metals in binary and ternary transition metal oxides [9,10]. The trend of increasing L_3/L_2 ratio with decreasing oxidation state is consistently reported in the literature [8,10–12]. The L_3/L_2 area ratio values presented in Table 3 from Schmid and Mader [12] agree closely with values measured in this work on the reference compounds MnO, Mn_2O_3, Mn_3O_4 bulk, Mn_3O_4 nano and MnO_2.

Table 1 – Energy positions (in eV) for the major features identified over the ELNES energy domain of the O–K edges displayed in Fig. 3. Note: error in energy values is ±0.1 eV.

Position (eV)	MnO	Mn_3O_4–bulk	Mn_3O_4–nano	Mn_2O_3	MnO_2
a a_1	535.2	532.3	532.4	532.5	531.5
a'_1		533.1	533.2		
a_2	536.6	535.4	535.5	533.6	533.9
a_3				535.4	
b	541.2	542.6	542.7	544.7	546
c	546.7	549.6	549.7	559.1	556.9
d	559.8	562.6	562.7		

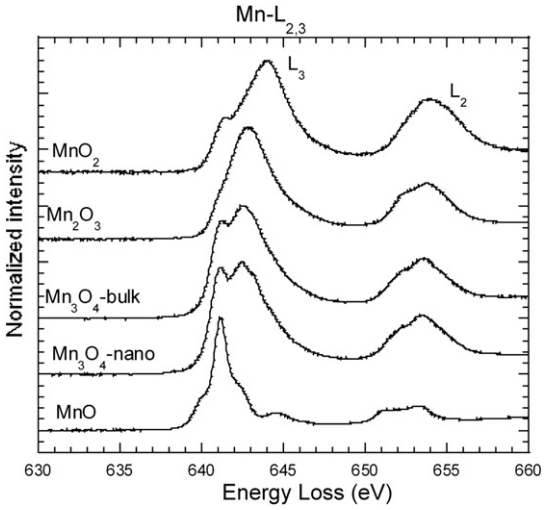

Fig. 4 – Manganese $L_{2,3}$ edge spectra from five studied oxides after deconvolution of multiple loss events and background subtraction.

The EELS Mn–L edges of MnO, MnO_2 and O–K edges of MnO, Mn_2O_3 and MnO_2 are equivalent in energy resolution to existing X-ray data [13] and show better resolution than in any published EELS data. The TEM/EELS with improved energy resolution gives access to the same information as the synchrotron. This opens up the exciting possibility of studying the electronic structure of materials with the same physical method either in a surface-sensitive (XAS) or in a bulk sensitive (EELS) mode with complete geometric structure information (SAED, HREM) and nanometer lateral resolution.

3.3. *Oxidation States*

For the nano-sized Mn_3O_4, other information is necessary to describe fully the electronic structure as the oxidation states. The ability of EELS to observe variations in oxidation state at high spatial resolution is studied in two different samples: one nano-Mn_3O_4 and other Mn_3O_4 bulk (micrometer size). Fig. 5 illustrates a typical $L_{2,3}$ edge from the first sample. This Mn–L_3 edge can be interpreted by consideration of its crystal structure and can be represented by the formula Mn^{2+} Mn^{3+} (2) O_4 with an ideal Mn^{3+}–Mn^{2+} ratio of 2:1. In fact, the L_3 lines are clearly composed of two main peaks that roughly correspond to the contribution of Mn^{2+} and Mn^{3+}. To achieve a more quantitative determination of redox state using Mn–$L_{2,3}$ reference spectra of both MnO and Mn_2O_3, these two

Table 2 – Energies (eV) of the Mn L_3 and L_2 edge peak maximum for oxide spectrum. Note: error in energy values is ±0.1 eV.

	L_3 main peak (eV)	L_2 main peak (eV)
MnO	641.2	653.2
Mn_3O_4 bulk	642.5	653.5
Mn_3O_4 nano	642.5	653.5
Mn_2O_3	642.8	653.7
MnO_2	644	653.7

Table 3 – comparison of the integrated L_3/L_2 ratio on the five manganese oxides of this study compared to the work of Schmid and Mader.

	I (L_3)/I(L_2) ratio	I (L_3)/I(L_2) ratio from [12]
MnO	4 (±0.2)	3.9 (±0.3)
Mn_3O_4 bulk	2.8 (±0.1)	2.8 (±0.2)
Mn_3O_4 nano	2.9 (±0.1)	
Mn_2O_3	2.5 (±0.05)	2.4 (±0.1)
MnO_2	2.1 (±0.05)	2 (±0.1)

reference spectra are also gathered in Fig. 5 and correspond to references of pure Mn^{2+} and Mn^{3+}, respectively. The fine structure of nano-Mn_3O_4 can be reconstructed by a linear combination of the two references MnO and Mn_2O_3. The scaling factors of the fitted spectra represented by dashed line in Fig. 5 are 0.4 and 0.6 of MnO and Mn_2O_3 (Mn^{3+}–Mn^{2+} ratio of 1.5) whereas for the Mn_3O_4 bulk, the scaling factors are 0.33 and 0.67 of MnO and Mn_2O_3 (not represented here—ideal Mn^{3+}–Mn^{2+} ratio). For the linear combination of the reference spectra, the values for each spectrum were obtained with an error of ±0.01 which correspond to an error bar of ±2%. The Mn^{3+}/Mn^{2+} ratio error is about ±0.01 showing the difference between the nano and bulk sample.

For nano-Mn_3O_4, the EELS spectrum is similar to the edge shape recorded by XANES [14] and ELNES [9], representative spectra correspond to the ideal Mn^{3+}–Mn^{2+} ratio of 2, although experimentally synthesized Hausmannite was found to have Mn^{3+}–Mn^{2+} ratios varying from 1.5 to 3 [15]. This different Mn^{3+}–Mn^{2+} ratio obtained for Mn_3O_4 bulk and nano can be related to the size of particles: one is nanometre size whereas the other is micrometre but also to the presence of vacancies on tetrahedral sites as mentioned by Kaczmarek and Wolska [15]. For $Mn^{3+}/Mn^{2+} \leq 2.4$ the vacancies are created merely on the tetrahedral sites whereas for $Mn^{3-}/Mn^{2+} > 2.4$ the excess of vacancies is distributed at random over the tetrahedral and octahedral sites.

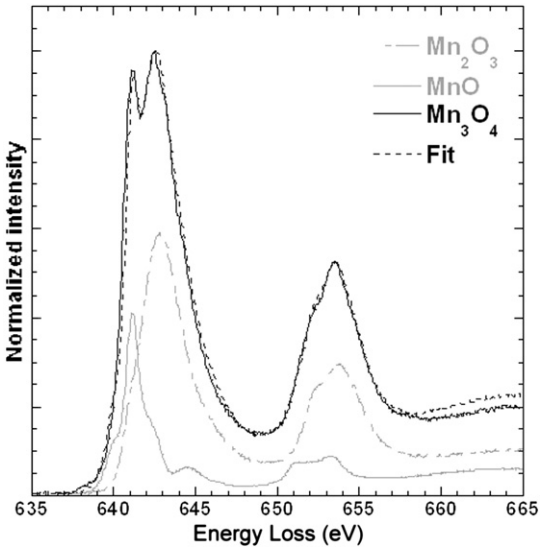

Fig. 5 – Manganese $L_{2,3}$ edges spectra of the two reference spectra MnO, Mn_2O_3 and the nano-Mn_3O_4 combined with the fitted spectrum to determine the oxidation state.

This study shows how complementary experimental techniques such as XRD, TEM and EELS can be used to investigate manganese oxides. XRD and TEM enable us to conclude that hydrophilic Mn_3O_4 synthesized is a crystallized Hausmannite oxide described by a $I4_1/amd$ space group and that it consists of sphere-shaped particles having an average diameter of 10–20 nm. By EELS investigations, we have found a Mn^{3+}/Mn^{2+} ratio of 1.5 showing the presence of vacancies on the tetrahedral sites. These complementary techniques are essential to determine clearly the structure of manganese oxides.

4. Conclusion

The as-made nano-Mn_3O_4 material was studied by complementary techniques such as XRD, TEM and HREELS in order to determine the degree of crystallinity, the monocrystalline character and the narrow grain size of this sample. EELS investigation gave access to a Mn^{3+}/Mn^{2+} ratio of 1.5, i.e. slightly lower than the theoretical value of 2 for bulk Hausmannite. This difference was related to the presence of vacancies on the tetrahedral sites in the nano-Mn_3O_4. In addition, it must be emphasized that HREELS technique enables us to rule out any compositional and valence inhomogeneity of these powders at nanometer scale.

Acknowledgment

We thank Dr P. Kooymann for her help at the National Centre for HREM in Delft, The Netherlands.

REFERENCES

[1] Hebert C, Willinger M, Su DS, Pongratz P, Schattschneider P, Schlogl R. Oxygen K edge in vanadium oxides: simulations and experiments. Eur Phys J B 2002;28:407–14.
[2] Gloter A, Serin V, Turquat C, Cesari C, Leroux C, Nihoul G. Vanadium valency and hybridization in V-doped hafnia investigated by electron energy loss spectroscopy. Eur Phys J B 2001;22:179–86.
[3] Gibot P, Laffont L. Hydrophilic and hydrophobic nano-sized Mn_3O_4. J Solid State Chem 2007;180:695–701.
[4] Garvie Laurence AJ, Craven Alan J, Brydson R. Use of electron-energy loss near-edge fine structure in the study of minerals. Am Mineralog 1994;79:411–25.
[5] Grunes LA, Leapman RD, Wilker CN, Hoffmann R, Kunz AB. Oxygen K near-edge fine structure: an electron-energy-loss investigation with comparisons to new theory for selected 3d transition-metal oxides. Phys Rev B 1982;25:7157–73.
[6] de Groot FMF, Grioni M, Fuggle JC, Ghijsen J, Sawatzky GA, Petersen H. Oxygen 1s X-ray absorption edges of transition metal oxides. Phys Rev B 1989;40:5715–23.
[7] Rez P, Weng X, Ma H. The interpretation of near-edge structure. Microsc Microanal Microstruct 1991;2:143–51.
[8] Kurata H, Lefèvre E, Colliex C, Brydson R. Electron-energy-loss near edge structures in the oxygen L-edge spectra of transition-metal oxides. Phys Rev B 1993;47(13):763–8.

[9] Paterson JH, Krivanek OL. Elnes of 3d transitions oxides: II variations with oxidation states and crystal structure. Ultramicroscopy 1990;32:319–25.
[10] Rask JH, Miner BA, Buseck PR. Determination of manganese oxidation states in solids by electron energy loss spectroscopy. Ultramicroscopy 1987;21:321–6.
[11] Botton GA, Appel CC, Horsewell A, Stobbs WM. Quantification of the EELS near-edge structure to study Mn doping in oxides. J Microsc 1995;180:211–6.
[12] Schmid HK, Mader W. Oxidation states of Mn and Fe in various compound oxide systems. Micron 2006;37: 426–32.
[13] Gilbert B, Frazer BH, Belz A, Conrad PG, Nealson KH, Haskel D, et al. Multiple scattering calculations of bonding and X-ray absorption spectroscopy of manganese oxides. J Phys Chem A 2003;107:2839–47.
[14] Cressey G, Henderson CMB, Vand der Laan G. Use of L edge X-ray-absorption spectroscopy to characterise multiple valence states of 3d transition metals: a new probe for mineralogist and geochemical research. Phys Chem Miner 1993;20:111–9.
[15] Kaczmarek J, Wolska E. Cation and vacancy distribution in nonstoichiometric hausmanite. J Solid State Chem 1993;103: 387–93.